THE AMERICAN SOCIETY OF MECHANICAL ENGINEERS
Three Park Avenue, New York, N.Y. 10016-5990

99-GT-385






# SHUNTED PIEZOELECTRIC CONTROL OF AIRFOIL VIBRATIONS

Charles J. Cross
Air Force Research Laboratory
Propulsion Directorate
WPAFB, OH 45433

Sanford Fleeter
School of Mechanical Engineering
Purdue University
West Lafayette, IN 47907

Presented at the International Gas Turbine & Aeroengine Congress & Exhibition
Indianapolis, Indiana — June 7–June 10, 1999

## ABSTRACT

The application of shunted piezoelectric elements to provide passive structural damping is investigated by means of experiments performed in the Purdue High Speed Axial Compressor Research Facility. Piezoelectric elements are bonded to three airfoils in the stator row. This airfoil is excited by the wakes generated by an upstream rotor. As the wakes drive the airfoil vibrations, the piezoelectrics experience a strain and in response produce an electric field. Tuned electrical circuits connected to the piezoelectrics as shunts dissipate this electrical energy, with multiple shunting techniques utilized. This electrical energy dissipation and the corresponding reduction in the airfoil mechanical energy result in a reduction in the magnitude of the resonant vibrations. Thus, these passive vibration control experiments demonstrate that shunted piezoelectrics have significant damping capability and could be practical for the elimination or minimization of gas turbine blading flow induced vibrations.


## NOMENCLATURE

- $d$ - piezoelectric strain constant
- $g$ - charge density per applied strain
- $k$ - electromechanical coupling coefficient
- $r$ - electric damping ratio
- $r^{opt}_{TF}$ - optimal electric damping ratio
- $s$ - elastic compliance
- $s$ - Laplace operator
- $A$ - area of element face
- $C^{T}_{pi}$ - capacitance between parallel faces of piezoelectric element
- $D$ - electrical displacement vector
- $E$ - electrical field vector
- $F$ - applied force
- $K$ - spring stiffness
- $K^{E}_{P}$ - spring stiffness of piezoelectric elements
- $K_{ij}$ - generalized electromechanical coupling coefficient
- $K_{TOT}$ - stiffness of entire system
- $I$ - current
- $L_i$ - length of element
- $L$ - inductance
- $M$ - mass
- $R$ - resistance
- $S$ - strain vector
- $T$ - material stress vector
- $U$ - strain energy
- $V$ - voltage
- $Y^{D}$ - admittance of piezoelectric element, open circuit
- $Y^{EL}$ - total admittance of shunted piezoelectric

$Y^{SU}$ - admittance of electrical shunt
$Z$ - impedance
$\gamma$ - non-dimensional frequency
$\delta$ - non-dimensional tuning parameter
$\delta^{opt}_{TF}$ - optimal tuning parameter
$\varepsilon$ - permittivity
$\eta$ - loss factor
$\eta^{TOT}$ - total loss factor of system
$\rho$ - non-dimensional frequency
$\omega^{D}_{n}$ - open circuit natural frequency
$\omega^{E}_{n}$ - short circuit natural frequency

## INTRODUCTION

Each new generation of gas turbine engines is required to be lighter and more powerful. The design approach to achieving this increased thrust-to-weight ratio involves increasing the flow through the engine and utilizing fewer parts. This is accomplished with new compressor designs with higher tip speeds, lower aspect ratio blading, more closely spaced blade rows and fewer stages. As a result, advanced compressors utilize extremely thin low aspect ratio airfoils which when combined with the increased flow through the engine, result in a significant increase in the aerodynamic loading and corresponding high steady state stresses. Also, the mechanical damping is considerably reduced in newer rotor designs, particularly those with integral blade-disk configurations (blisks) and in those without shrouds. As a result, the low aspect ratio blading of advanced compressors have significant unsteady flow induced vibration problems, both flutter and forced response.

Flow induced vibrations of turbomachinery blading are the cause of high cycle fatigue (HCF) and the need for both unscheduled and scheduled maintenance. Minimization of the response to aerodynamic forcing functions can reduce or even alleviate the need for costly repairs and diminish the possibility of HCF. With new turbine engine component concepts and stringent design requirements, innovative concepts for controlling airfoil vibrations and minimizing their destructive effects must be explored. This need for new solutions is evident since many of the traditional solutions minimize HCF but also negate the performance improvements of the new designs. Additionally, as older engines are modified to meet increased performance demands, after-design solutions must be available to address new resonant problems without a need for component replacement.

Piezoelectric materials represent a relatively new approach to vibration suppression and control. By their nature, piezoelectric materials are well suited for use as dampers and control elements. When an electric current is applied to the piezoelectric material, a corresponding strain is produced within the material that causes the production of an electrical voltage. Conversely, straining a piezoelectric material causes the production of an electrical voltage.

In general, a piezoelectric ceramic material, either lead zirconate titanate (PZT) or polyvinylidend fluoride (PVDF) is mounted onto or embedded in a host structure and is used as a sensor, actuator, or both a sensor and actuator. As the attached structure vibrates, the piezoelectric experiences a strain and in response produces an electric field. Manipulation of this energy transfer can result in control and reduction of the vibration characteristics of the structure. For active vibration control using piezoelectrics, a complex system for sensing, control and feedback are necessary. Smart structures of this type have been considered by Crawley and deLuis [1], Poh and Baz [2], and Bailey and Hubbard [3].

Piezoelectric materials can also be used as components of a passive damping system,

thereby avoiding complex control and feedback systems. Piezoelectrics provide passive damping by using electrical impedance as a dissipating shunt. Namely, the electric field generated by the strain of the piezoelectric bonded to a vibrating host structure is dissipated by the electrical shunt. This conversion of mechanical energy to electrical energy results in a reduction in the resonant vibrations.

Resistive and resonant electrical shunting have been considered. In resistive shunting, a resistor is placed in parallel with the piezoelectric. The resistor provides an additional energy loss in the system, thereby dissipating current provided by the piezoelectric. The implementation of a resistor shunt has been shown to be similar to increasing the viscoelastic damping of the system. In resonant shunting, an L-R-C circuit is formed by adding an inductor and resistor in series with the inherent capacitance of the piezoelectric. The circuit produces a damped electrical resonance. The resonance can be tuned so that the piezoelectric acts as a damped vibration absorber. Multimode passive dampers are achieved by adding additional L-R-C circuits to the initial shunt, thereby enabling multimode suppression with a single piezoelectric device.

Hollkamp and Starchville [4] and Hagood and von Flotow [5] performed experiments demonstrating shunted piezoelectrics to provide damping to control vibrations of cantilever beams. The analytical derivation of a passive piezoelectric damper was developed by Hagood and von Flotow and is the basis for both of these passive damping experiments. They first derived the mechanical impedance of a piezoelectric material, and then developed mathematical expressions for both resistive and resonant circuit shunting. In these, beam structures or a complex structure of beam elements were the basis for the application. Also, plate structures subjected to aerodynamic loading were not considered.

With new component concepts and stringent design requirements, innovative techniques for controlling gas turbine engine airfoil vibrations must be explored. In this regard, critical vibration modes are associated with the blade aspect ratio. High aspect ratio blades resemble beams, with the resulting response typically occurring in the lower order modes, i.e., simple bending and torsion. However, the vibration characteristics of low aspect ratio blades more closely resemble plates than beams. As a result, complex higher order modes, specifically chordwise bending modes, are significant for flow induced vibrations of advanced blade rows. Unfortunately, complex higher order modes inherently have little damping, either mechanical or aerodynamic. As a result, techniques to control the flow-induced vibrations with emphasis on higher order modes are needed.

This paper addresses this fundamental need to investigate new techniques for control of low aspect ratio turbomachine blade row chordwise bending mode flow induced vibrations. Thus, the application of piezoelectric materials as passive and active damping elements on gas turbine engine airfoils is considered. Specifically, the application of shunted piezoelectric elements to provide passive structural damping is investigated by means of a series of experiments performed in the Purdue High Speed Axial Compressor Research Facility. Piezoelectric elements are bonded to three airfoils in the stator row. The airfoils are excited by the wakes generated by an upstream rotor. As the wakes drive the airfoil vibrations, the piezoelectrics experience a strain and in response produce an electric field. Tuned electrical circuits

connected to the piezoelectrics as shunts dissipate this electrical energy. This electrical energy dissipation and the corresponding reduction in the airfoil mechanical energy result in a reduction in the magnitude of the resonant vibrations.

## PIEZOELECTRIC MODEL AND THEORY

Piezoelectric materials have the ability to transform electrical energy to mechanical energy and visa versa. Thus, they can provide passive damping by using electrical impedance as a dissipating shunt. This is accomplished by bonding a piezoelectric element to a structure such as a plate or beam. As the structure vibrates, the piezoelectric experiences a strain and in response produces an electric field. The electrical shunt in turn dissipates the electrical energy, thereby reducing the systems mechanical energy. The conversion of mechanical energy to electrical energy causes a reduction in the resonant vibrations of the structure.

Figure 1 illustrates a thin piezoelectric material element representing those that could be bonded to or embedded in surface of an airfoil.

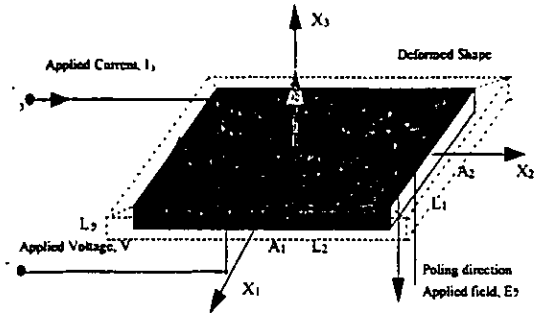


Figure 1. Piezoelectric Element Model

In this model, direction "3" is the direction through which the electric field and current act on the element, or the poling direction, and is perpendicular to directions "1" and "2" which lie along the surface of the host structure. It is generally assumed that the properties in the "1" and "2" directions are isotropic, and symmetry is used throughout the derivation. An understanding of the relationship between the deformed shape of the piezoelectric and its electrical response allows for an analysis of the vibratory motion of the airfoil by coupling its motion to that of the attached piezoelectric element.

To develop this coupling of electrical and mechanical properties, three constitutive relationships are defined. The constant "d" is the piezoelectric strain constant and is defined as the relation between material strain and the applied field. The constant "g" represents the relation between charge density and applied strain. The constant "k" is the electromechanical coupling term, which defines the electrical-mechanical energy transfer properties of the material. Numerically, the square of k is equal to the ratio of electrical energy, which is converted to mechanical energy to the input electrical energy. Since complete transfer is not possible, $k^2$, and therefore k is always less than one.

The general expression for the material constants of a linear piezoelectric is

$$\begin{bmatrix} \mathbf{D} \\ \mathbf{S} \end{bmatrix} = \begin{bmatrix} \boldsymbol{\varepsilon}^T & \mathbf{d} \\ \mathbf{d}_t & \mathbf{s}^E \end{bmatrix} \begin{bmatrix} \mathbf{E} \\ \mathbf{T} \end{bmatrix} \qquad (1)$$

where **D** is the electrical displacement vector (charge/area), **E** is the electrical field vector, **S** is the strain vector (volts/meter), **T** is the material stress vector (force/area), $\varepsilon$ is the permittivity (farad/meter), **s** is the elastic compliance (meter$^2$/newton), and **d** is the piezoelectric strain constant.

The vectors **D** and **S** are

$$\mathbf{D} = \begin{bmatrix} D_1 \\ D_2 \\ D_3 \end{bmatrix} = \begin{bmatrix} \varepsilon_1 E_1 + d_{15} T_5 \\ \varepsilon_1 E_2 + d_{15} T_4 \\ \varepsilon_3 E_3 + d_{31}(T_1 + T_2) + d_{33} T_3 \end{bmatrix}$$

$$\mathbf{S} = \begin{bmatrix} S_1 \\ S_2 \\ S_3 \\ S_4 \\ S_5 \\ S_6 \end{bmatrix} = \begin{bmatrix} s_{11}^E T_1 + s_{12}^E T_2 + s_{13}^E T_3 + d_{31} E_3 \\ s_{11}^E T_2 + s_{12}^E T_1 + s_{13}^E T_3 + d_{31} E_3 \\ s_{13}^E (T_1 + T_2) + s_{33}^E T_3 + d_{33} E_3 \\ s_{44}^E T_4 + d_{15} E_2 \\ s_{44}^E T_5 + d_{15} E_1 \\ s_{66}^E T_6 \end{bmatrix} \quad (2a,b)$$

and the **E** and **T** vectors conform to standard nomenclature for stress and electrical vectors.

$$\mathbf{E} = \begin{bmatrix} E_1 \\ E_2 \\ E_3 \end{bmatrix} \qquad \mathbf{T} = \begin{bmatrix} T_{11} \\ T_{22} \\ T_{33} \\ T_{23} \\ T_{13} \\ T_{12} \end{bmatrix} \quad (2c,d)$$

where the superscript T denotes that the property was measured under constant stress conditions and the superscript E that the property was measured in a constant electrical field.

The first equation of matrix Equation 1 represents the direct piezoelectric effect, or the creation of an electrical charge due to the application of a stress to the material. The second equation represents the converse effect or a stress resulting from the application of an electrical charge.

To perform an analysis using the traditionally defined concepts of admittance and impedance, the electrical field vector (E) and the electrical displacement vector (D) must be replaced by current (I) and voltage (V). Using standard definitions,

$$V_i = \int_0^{L_i} \mathbf{E} \cdot dx_i \qquad I = \int_{A_i} \mathbf{D} \cdot da_i \quad (3)$$

and assuming uniform fields and displacements throughout the piezoelectric, a transfer to the Laplace domain yields

$$\mathbf{V}(s) = \mathbf{L} \cdot \mathbf{E}(s) \qquad \mathbf{I}(s) = s\mathbf{A} \cdot \mathbf{D}(s) \quad (4)$$

where **L** is the diagonal matrix of the lengths of the piezoelectric element in the $i^{th}$ direction, **A** is the diagonal matrix of the areas of the surfaces of the piezoelectric element orthogonal to the $i^{th}$ direction, and s is the Laplace parameter.

Taking the Laplace transform of Equation 1 in conjunction with these definitions leads to the following expression for the piezoelectric in terms of external current and the applied voltage.

$$\begin{bmatrix} \mathbf{I} \\ \mathbf{S} \end{bmatrix} = \begin{bmatrix} s\mathbf{A}e^T\mathbf{L}^{-1} & s\mathbf{A}\mathbf{d} \\ \mathbf{d}_t\mathbf{L}^{-1} & \mathbf{s}^E \end{bmatrix} \begin{bmatrix} \mathbf{V} \\ \mathbf{T} \end{bmatrix} \quad (5)$$

Defining the capacitance between perpendicular surfaces in the $i^{th}$ direction as

$$C_{pi}^T = \frac{A_i \varepsilon_i^T}{L_i} \quad (6)$$

and grouping the components into a $\mathbf{C}_p^T$ matrix, Equation 5 can be written in the form:

$$\begin{bmatrix} \mathbf{I} \\ \mathbf{S} \end{bmatrix} = \begin{bmatrix} \mathbf{Y}^D(s) & s\mathbf{A}\mathbf{d} \\ \mathbf{d}_t\mathbf{L}^{-1} & \mathbf{s}^E \end{bmatrix} \begin{bmatrix} \mathbf{V} \\ \mathbf{T} \end{bmatrix} \quad (7)$$

where $\mathbf{Y}^D(s) = s\mathbf{C}_p^T$ and is defined as the open circuit admittance of the piezoelectric. The open circuit admittance relates the voltage applied across the materials electrodes to the external current input to the piezoelectric. A complete understanding of piezoelectric theory can be found in Jaffe, Cook and Jaffe [6].

**Piezoelectric Shunting:** For shunting, a passive electrical circuit is placed between the electrodes of the piezoelectric element. The circuit is parallel to the capacitance of the piezoelectric and therefore the total admittance of the device, $\mathbf{Y}^{EL}$, is the sum of the individual admittance from the device, $\mathbf{Y}^D$, and the shunt, $\mathbf{Y}^{SU}$, or $\mathbf{Y}^{EL} = \mathbf{Y}^D + \mathbf{Y}^{SU}$.

Only the equations needed to correctly size and apply shunting circuits will be presented herein, with a complete derivation of the piezoelectric shunting equations found in Hagood and von Flotow.

To find the overall effect on the system, or effective impedance of the piezoelectric shunt, their properties must be combined with the properties of the other damping elements acting on the system. Using the method of combining viscoelastic damping elements, the relationship between the loss factor of damping components and the loss factor of the overall structure can be expressed as an average of the component loss factors multiplied by their fraction of the total strain energy. Defining $U_i$ as the strain energy in the $i^{th}$ component of the structure, the total loss factor is numerically expressed as

$$\eta^{TOT} = \sum_{i=1}^{n} \frac{\eta_i U_i}{\sum_{i=1}^{n} U_i} \tag{8}$$

Maximizing the loss factor for the piezoelectric device does not necessarily maximize the loss factor for the structure. The total damping of the system consists of a combination of all damping methods in the system, weighted by their fraction of the strain energy dissipated.

One method of determining the system damping is to consider the piezoelectric shunt as a viscoelastic material with frequency dependent properties. For the resistive shunted device, the properties are similar to those of a linear solid. However, for the resonant shunted device, the properties are non-linear functions of frequency and the tuning parameters. As a result, a prior knowledge of the properties must exist to effectively predict the effect of the resonant shunt on the system.

The second method of obtaining the system damping is to represent the system by a simple 1-DOF system including the piezoelectric device. The mass and stiffness of this 1-DOF system can represent a particular mode of a multi-DOF system. In the Laplace domain, the modal velocity of the system can be expressed as

$$v(s) = \frac{F(s)}{Ms + \left(\frac{K}{s}\right) + Z_{ij}^{RES}(s)} \tag{9}$$

where F(s) is the magnitude of the forcing function and Ms, K/s, and $Z_{ij}^{RES}(s)$ are the impedances associated with the modal mass, stiffness, and resistive shunt respectively. The impedance of an element is the inverse of its admittance.

Non-dimensionalization and reduction results in the following transfer function.

$$\frac{x}{\left(F / K_{tot}\right)} = \frac{(r\gamma + 1)}{(r\gamma^3 + \gamma^2 + r(1 + K_{ij}^2)\gamma + 1} \tag{10}$$

where $K_{tot}$ is the total modal stiffness of the system, $K_{ij}^2 = \left(\frac{K_{ij}^E}{K + K_{ij}^E}\right)\left(\frac{k_{ij}^2}{1 - k_{ij}^2}\right)$ is the generalized electromechanical coupling coefficient, $\omega_n^E = \sqrt{\frac{(K + K_{ij}^E)}{M}}$, and $\gamma = \frac{s}{\omega_n^E}$ and $r = R_i C_{pi}^S \omega_n^E = \rho|_{\omega=\omega_n^E}$ are the nondimensional frequency and the electric damping ratio.

The generalized electromechanical coupling coefficient describes the fraction of the modal strain energy, which is converted into electrical energy, and therefore serves as a direct measurement of the shunt's effect on the system. A miscalculation of this energy fraction greatly affects the circuit sizing. Noting that the natural frequency of the structure changes as the damping due to the piezoelectric elements varies, the effect of short versus open shunting circuit can be seen in the frequency of vibration. The open circuit and short circuit natural frequencies are

$$\omega_n^D = \sqrt{\frac{\left\{K + \frac{K_p^E}{1 - k_{ij}^2}\right\}}{M}} \tag{11}$$

$$\omega_n^E = \sqrt{\frac{\left\{K + K_p^E\right\}}{M}} \qquad (12)$$

where K is the effective stiffness of the underlying structure, $K_p^E$ is the effective stiffness of the piezoelectric elements, and M is the mass of the system, the generalized electromechanical coupling coefficient can be determined experimentally.

Combining Equations 11 and 12, the generalized electromechanical coupling coefficient is

$$K_{ij}^2 = \frac{\left(\omega_n^D\right)^2 - \left(\omega_n^E\right)^2}{\left(\omega_n^E\right)^2}. \qquad (13)$$

Utilizing this experimental method of determining the generalized electromechanical coupling coefficient, most variables due to construction of the system can be taken into account. With the various natural frequencies known, and thus the generalized electromechanical coupling coefficient determined, the shunting circuit can be designed.

Due to the nonlinear dependence of the resonant shunted effective natural properties on the frequency and tuning parameter, optimization by considering energy dissipation is difficult. Hence, optimization must be based on another criteria. A common method in the transfer function technique wherein the transfer function is evaluated at an electric damping ratio of zero, r = 0, and where the ratio goes to infinity. A quadratic expression is found for their intersection points. In proof mass dampers, these points are termed the S and T locations. From the sum of the roots of this quadratic expression, the following optimal tuning parameter is determined.

$$\delta_{TF}^{opt} = \sqrt{1 + K_{ij}^2} \qquad (14)$$

When the optimal tuning parameter is specified, the optimal damping in the electrical circuit can be determined. A convenient method for optimization sets the amplitude of the transfer function at the desired operating frequency to that of the system at the S and T points. The resulting analysis shows that the optimum circuit damping is

$$r_{TF}^{opt} = \frac{1.414 K_{ij}}{1 + K_{ij}^2}. \qquad (15)$$

**Shunting Circuit Impedance:** In resistive shunting, a resistor is placed in the circuit parallel to the inherent capacitance of the piezoelectric element. The resistor provides a means for dissipation of the electrical energy developed through the vibration of the underlying structure.

Returning to the nondimensional electrical impedance and identifying that the shunted impedance is the value of the resistor

$$Z_i^{SU}(s) = R_i \qquad (16)$$

the non-dimensional electrical impedance for resistive shunting is

$$\bar{Z}_i^{EL}(s) = \frac{R_i C_{pi}^T s}{\left(R_i C_{pi}^T s + 1\right)} \qquad (17)$$

Substituting into the piezoelectric nondimensional mechanical impedance, the nondimensional impedance of a resistive shunted piezoelectric is determined.

$$\bar{Z}_{ij}^{RES}(s) = 1 - \frac{k_{ij}^2}{(1 - i\rho_i)} \qquad (18)$$

where $\rho_i = R_i C_{pi}^S \omega = \sqrt{1 - k_{ij}^2}$ is the non-dimensional frequency.

In resonant circuit shunting, a resistor and an inductor are placed in series with the inherent capacitance of the piezoelectric element to create an L-R-C circuit. The electrical resonance of the new circuit can be tuned to the frequency of the mechanical vibration. The electrical resonance greatly increases the modal damping ratio. It has been shown that the effect of resonant

piezoelectric shunting is similar to a mass damper or a resonant vibration absorber.

The electrical impedance of the resonant shunt is a function of both the resistor and inductor values. Substituting into the nondimensional mechanical impedance leads to

$$\bar{Z}_{ij}^{RES}(s) = 1 - k_{ij}^2\left(\frac{\delta^2}{\gamma^2 + \delta^2 r\gamma + \gamma^2}\right) \qquad (19)$$

where r is the damping parameter, $\delta = \frac{\omega_e}{\omega_n}$ is the nondimensional tuning frequency, $\gamma = \frac{\omega}{\omega_n}$ is the nondimensional frequency and

$$\omega_n^E = \frac{1}{\sqrt{LC_{pi}^S}} \qquad (20)$$

is the electrical resonant frequency.

**Shunting Circuit Sizing:** With the relationships between the electrical and mechanical properties of the shunted system determined, the following summarizes the equations needed to practically apply the technique. Before a shunt can be applied, the basic properties of the system, piezoelectric elements, and their interactions must be understood. The inherent capacitance of each piezoelectric element is determined.

$$C_{pi}^T = \frac{A_i \varepsilon_i^T}{L_i} \qquad (6)$$

The open and short circuit natural frequencies of the shunted system are determined experimentally. Using a vibration driver, the system is excited to determine its resonant response frequency with the piezoelectric elements. For the open circuit configuration, a peak voltage output from the piezoelectric elements can be used to determine the resonant location. For the short circuit configuration with the leads of the piezoelectric elements connected, a peak current reading is appropriate.

With these natural frequencies determined, the generalized electromechanical coupling coefficient is calculated.

$$K_{ij}^2 = \frac{\left(\omega_n^D\right)^2 - \left(\omega_n^E\right)^2}{\left(\omega_n^E\right)^2} \qquad (13)$$

The optimal tuning parameter and the circuit damping can now be determined.

$$\delta_{TF}^{opt} = \sqrt{1 + K_{ij}^2} \qquad (14)$$

$$r_{TF}^{opt} = \frac{1.414 K_{ij}}{1 + K_{ij}^2} \qquad (15)$$

For a resistive shunt, the required resistance is

$$\rho_i = R_i C_{pi}^S \omega = \sqrt{1 - k_{ij}^2} \qquad (18)$$

For a resonant shunt, the required inductor and resistor values are

$$\omega_n^E = \frac{1}{\sqrt{L_i C_{pi}^S}} \qquad (20)$$

$$r = R_i C_{pi}^S \omega_n^E = \rho\big|_{\omega=\omega_n^E} \qquad (10)$$

## AIRFOIL FORCED RESPONSE EXPERIMENTS

The application of shunted piezoelectric elements to provide passive structural damping to turbomachine blade rows is investigated by means of a series of experiments performed in the Purdue High Speed Axial Compressor Research Facility. Piezoelectric elements are bonded to three airfoils in the stator row. The airfoils are excited by upstream rotor generated wakes. The piezoelectrics experience a strain and in response produce an electric field, with tuned electrical circuits connected to the piezoelectrics as shunts designed to dissipate this electrical energy.

**Experimental Facility:** The piezoelectric damping experiments are

conducted in the Purdue High Speed Axial Compressor Research Facility, Figure 2, a stage and a half turbomachine featuring an inlet guide vane (IGV) row, a rotor, and a stator row. At a rotational speed of 20,000 rpm, the flow is transonic. The drive system consists of a 400 horsepower AC motor driving a variable speed magnetic clutch that in turn drives an 8:1 ratio gearbox, the output of which drives the compressor rotor. The flow rate through the facility is controlled by a butterfly valve in the discharge ducting.

aircraft engine high-pressure compressors. Both the IGV and stator vanes have controlled diffusion airfoil (CDA) profiles. The IGV is designed to deliver an inlet pre-swirl distribution to the rotor which varies from 110° at the root to 95° at the tip. The IGV's are 7% thick, with the maximum thickness at 39% chord, a total chord of 2.0 in. and the total camber varying from approximately 29° at the root to 9° at the tip.

The two-dimensional constant section stator vanes are 7% thick with the maximum

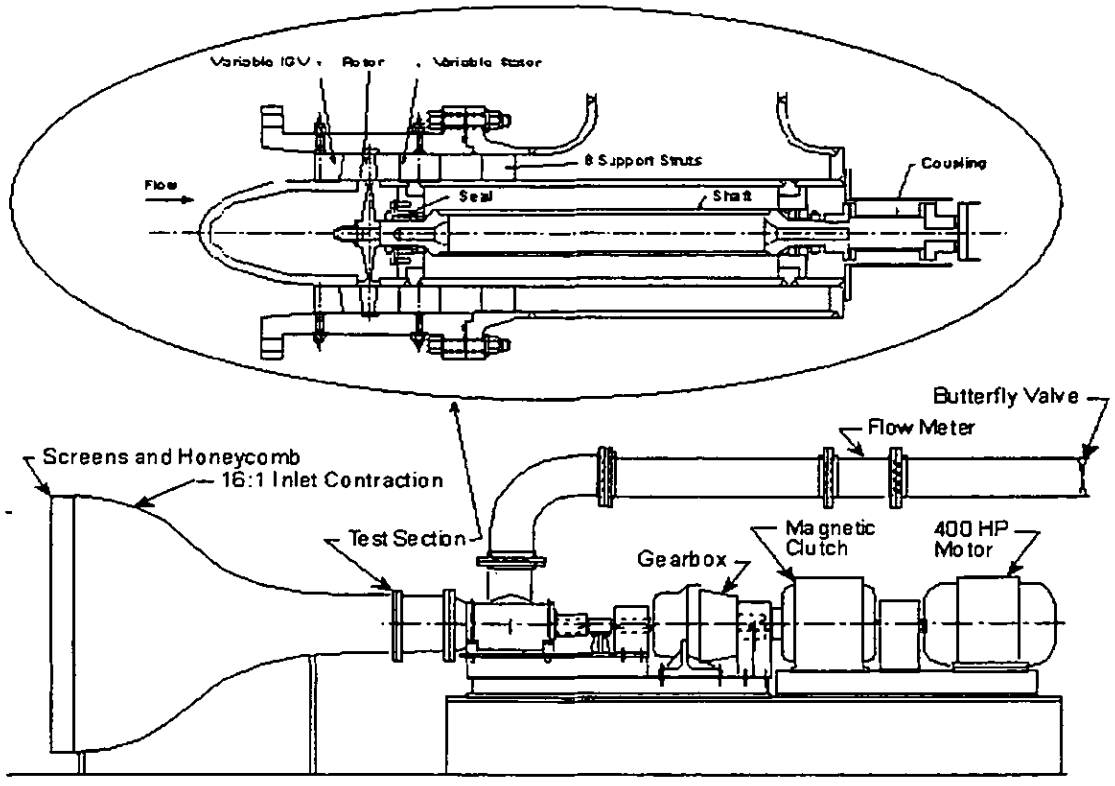


Figure 2. Purdue High-Speed Axial Compressor Research Facility

The compressor test section consists of an indexable variable stagger IGV followed by an aluminum rotor. The rotor airfoils are cast integrally with the disk, i.e. a blisk, and features 19 NACA 65 series airfoil profiles on circular arc meanlines. The IGV and stator vanes are representative of those used in the front stages of modern commercial

thickness at 39% chord, a 1.75 in. total chord, and 40° of total camber. A cross section of the stator vane is presented in Figure 3. Both the IGV and stator have 18 vanes, with a gap-chord ratio that varies linearly from 0.8 at the root to 1.2 at the tip. The IGV and stator vane stagger angle, as well as the IGV-rotor-stator axial spacing

are variable, with a minimum spacing of 1/4 in. (12.5% rotor chord) obtainable at the root. Both the IGV's and stator vanes are mounted on cantilevered trunnions, with the mounting arrangement such that the mechanical damping is kept to a minimum.

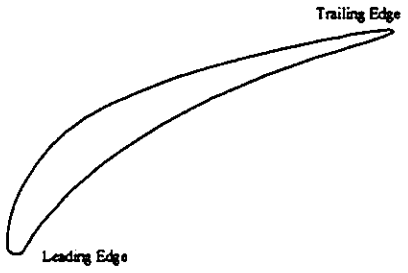


Figure 3. Stator Vane Cross Section Profile

strain area independently. For reference, the vanes with the same piezoelectric volume are known as the SPE vane for the vane with the single piezoelectric element and as the 2PE vane for the vane with the two piezoelectric elements. The third vane, with the larger piezoelectric volume is known as the LPE vane. The location and dimensions of the piezoelectric elements is presented in Figure 4.

**Shunted Piezoelectric Passive Vibration Control:** The piezoelectric stator airfoils are excited by the rotor wakes. The piezoelectric patches bonded to the airfoils are lead zirconate titanate G1195 manufactured by Piezo Systems Incorporated. The material properties of the individual patches are given in Table 1.

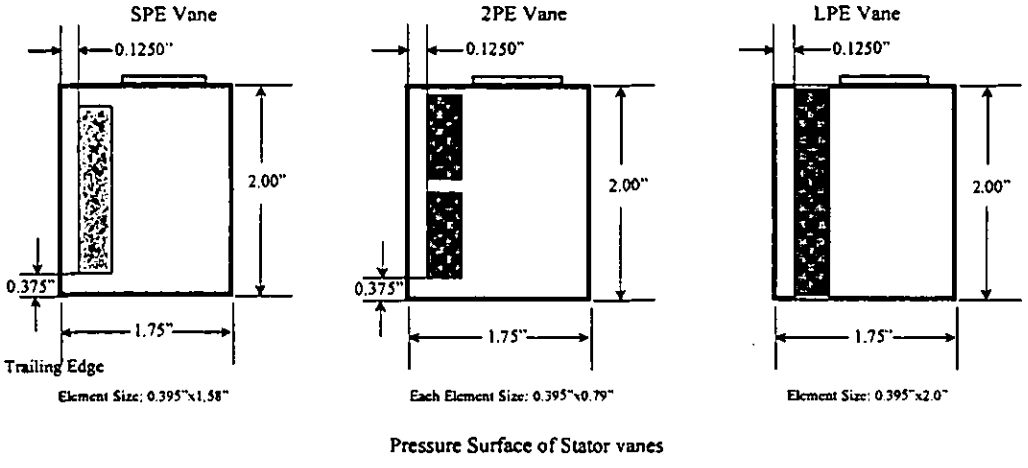


Figure 4. Location and Dimensions of Piezoelectric Elements

**Piezoelectric Airfoils:** Three vanes with bonded piezoelectric elements are evaluated. The volume of the piezoelectric elements are the same on two of the vanes, with a single large element bonded on one vane and two smaller elements mounted on the other. The third vane has a piezoelectric element approximately 20% larger extending completely across the span. For the two vanes with a single element, the piezoelectric element is placed to cross two nodal lines, whereas on the vane with two elements, each element acts across a large

| | | | |
|---|---|---|---|
| Composition | Lead Zirconate Titanate | | |
| Material Designation | G1195 | | |
| Relative Dielectric Constant | | | |
| $K_3$ | 1700 | $K_1$ | 1700 |
| Piezoelectric Strain Coefficient | | | |
| $d_{33}$ | $360*10^{-12}$ | Meters/Volt | |
| $d_{31}$ | $166*10^{-12}$ | Meters/Volt | |
| Piezoelectric Voltage Coefficient | | | |
| $g_{33}$ | $25*10^{-3}$ | Volt Meters/Newton | |
| $g_{31}$ | $11*10^{-3}$ | Volt Meters/Newton | |
| Coupling Coefficients | | | |
| $k_{33}$ | 0.69 | $k_{31}$ | 0.35 |
| Density | 7600 | $Kg/Meter^3$ | |
| Elastic Modulus | | | |
| $Y^E_{33}$ | $4.9*10^{10}$ | $Newtons/Meter^2$ | |
| $Y^E_{11}$ | $6.3*10^{10}$ | $Newtons/Meter^2$ | |

Table 1. Piezoelectric and Material Properties of G1195

Based on the vane dimensions, the effective capacitance of the piezoelectric elements for each configuration was determined. For the SPE and 2PE vanes, an effective capacitance of $2.79*10^{-8}$ Farads was calculated and for the LPE vane the capacitance was $3.532*10^{-8}$ Farads.

In applying the design criteria for the resonant shunting circuit, a critical issue arises in evaluating the generalized electromechanical coupling coefficient. As defined, the generalized electromechanical coupling coefficient $K_{ij}$ describes the fraction of the modal strain energy converted into electrical energy, and therefore is a direct measurement of the effect of the shunt on the system. As previously discussed, the miscalculation of this energy fraction greatly affects the circuit sizing. Noting that the natural frequency of the structure changes as the damping due to the piezoelectric elements varies, the effect of short versus open shunting circuits is seen in the frequency of vibration. Hence, the electromechanical coupling coefficient is determined experimentally.

With the open and short circuit airfoil natural frequencies measured, the general parameters needed to size the resonant shunting circuit can be calculated. Based on holographically recorded resonant frequencies, the generalized electromechanical coupling coefficient $K_{ij}$ for the SPE vane is determined to be 0.0031. For the 2PE vane, it is also 0.0031, and for the LPE vane it is 0.0032.

Assuming a value of 0.0031 for each case, the optimum circuit tuning parameter $\delta^{opt}$ for the vanes is 1.0015, and the optimum circuit damping, $r^{opt}$ is 0.0785. The variation in circuit tuning and circuit damping values based on generalized electromechanical coupling coefficients ranging from 0.0031 to 0.0032 is indistinguishable.

Based on the experimentally determined tuning parameter and circuit damping, the resistance and inductor values are calculated for the passive damping circuits. Based on the effective capacitance of the SPE and 2PE vanes, the required resistance for a resistive shunt is 6,900 Ω. With the resonant shunt, the required resistance and inductance are 530 Ω and 1.3 H. For the LPE vane, the required resistance for a resistive shunt is 5,500 Ω and for the resonant shunt, the required resistance and inductance is 435 Ω and 1.1 H.

## RESULTS

Experiments incorporating shunted piezoelectric elements to damp the vibratory motion of stator vanes are performed in the Purdue High Speed Compressor Facility. With the upstream rotor providing the aerodynamic forcing function excitation, shunted piezoelectric passive damping effectiveness is demonstrated. Finite element codes and laser holography were used to structurally and dynamically analyze the stator row with bonded piezoelectric elements. The analyses and data were evaluated to determine placement of strain gages and piezoelectric elements for sensing and damping of the airfoil vibrations.

For these experiments, three stator vanes with bonded piezoelectric elements are evaluated for passive flow induced vibration control with various passive electrical shunting circuits. A speed transient that crosses a stator resonant mode at 5,333 Hz is obtained for each configuration of vane and circuit. Due to the sharpness of the resonant excitation band for this mode, Figure 5, an extremely slow transient was utilized to capture the vane response. For the transient

extending from 15,000 rpm to 17,000 rpm, the rotor speed is increased at a rate of 25 rpm/second. Three transients are obtained for each vane: a baseline response with no circuit connected to the piezoelectric; a resistively shunted response; and a resonant shunted response. The effect of each circuit on the vane response is determined through strain gages located at the vane trailing edge and the electrical output of the piezoelectric elements.

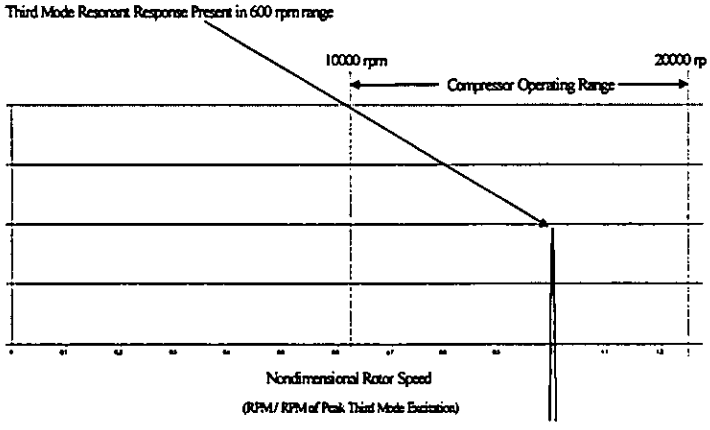


Figure 5. Resonant Condition with Respect to Compressor Operator Range

The baseline response and the effect of the resistive and resonant damping shunts on the vibratory response of the SPE vane, as determined by the strain gages, are presented in Figure 6.

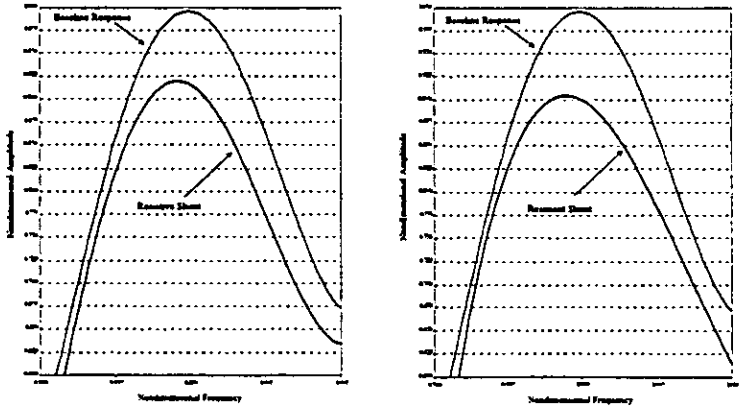

Figure 6. Piezoelectric Controlled Response of SPE Vane

For this vane, the decrease for both the resistive and resonant shunts is nearly identical. Application of the resistive shunt to the SPE vane results in an amplitude reduction of 8%, with a 9% reduction for the resonant shunt. Based on the relationship between the stress at the strain gage location and the maximum dynamic stress, a reduction of 9% in the strain gage signal is estimated to result in a reduction of 1.4 ksi in the maximum dynamic stress as compared to the baseline piezoelectric vane. Due to the increased stiffness of the piezoelectric vanes, the total reduction in maximum dynamic stress is estimated to be 4.8 ksi compared to the baseline steel vane.

The reduction in the electrical output of the piezoelectric element is approximately 17% for the resistive circuit and 19% for the resonant circuit. The electromechanical coupling relationship for this system verifies that these values correspond to the strain gage reduction values achieved.

The results near the resonant peak show the traditional peak shift that occurs as damping is increased. In each case, a system damping increase results in the resonant peak shifting to a lower frequency. Due to the sharpness of the peak, and the magnification needed to compare the peak responses, a valid estimate of the frequency shift is not practical. The half power bandwidth method estimate of the damping ratio of the baseline system is 0.0079. With the shunts attached to the airfoil, an increase in damping ratio is present for all circuits. The increase in damping ratio for the

resistive and resonant circuits is 0.0005 and 0.0007.

The baseline response and the effect of the resistive and resonant damping shunts on the vibratory response of the 2PE vane are presented in Figure 7.

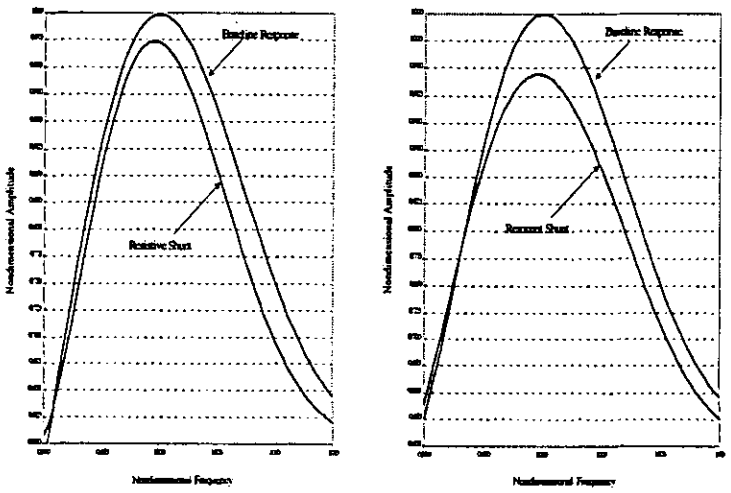

Figure 7. Piezoelectric Controlled Response of 2PE Vane

The decrease for the resonant shunt is approximately twice that of the resistive shunt. Application of the resistive shunt to the 2PE vane results in an amplitude reduction of 3%, with a 6% reduction for the resonant shunt. Based on the relationship between the stress at the strain gage location and the maximum dynamic stress, a reduction of 6% in the strain gage signal is estimated to result in a reduction of 0.9 ksi in the maximum dynamic stress as compared to the baseline piezoelectric vane. Due to the increased stiffness of the piezoelectric vanes, the total reduction in maximum dynamic stress is estimated to be 4.3 ksi compared to the baseline steel vane.

The reduction in the electrical output of the piezoelectric element is approximately 6% for the resistive circuit and 13% for the resonant circuit. As for the SPE vane, the electromechanical coupling relationship for this system verifies that these values correspond to the strain gage reduction values achieved. The half power bandwidth method estimate of the damping ratio of the baseline system is 0.0095. With the shunts attached to the airfoil, an increase in damping ratio is present for all circuits. The increase in damping ratio for the resistive and resonant circuits is 0.0004 and 0.0008.

The baseline response and the effect of the resistive and resonant damping shunts on the vibratory response of the LPE vane are presented in Figure 8.

Application of the resistive shunt to the LPE vane results in an amplitude reduction of 8%, with a resonant shunt reduction of approximately 11%. Based on the relationship between the stress at the strain gage location and the maximum dynamic stress, a reduction of 11% in the strain gage signal is estimated to result in a reduction of 1.7 ksi in the maximum dynamic stress as

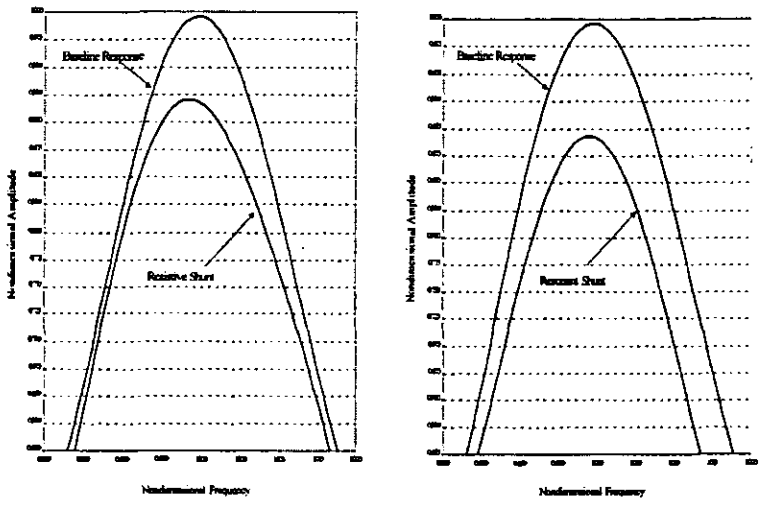

Figure 8. Piezoelectric Controlled Response of LPE Vane

compared to the baseline piezoelectric vane. Due to the increased stiffness of the piezoelectric vanes, the total reduction in maximum dynamic stress is estimated to be 5.1 ksi compared to the baseline steel vane.

The reduction in the electrical output of the piezoelectric element is approximately 17% for the resistive circuit and 23% for the resonant circuit. Once again, the electromechanical coupling relationship for this system verifies that these values correspond to the strain gage reduction values achieved. The half power bandwidth method estimate of the damping ratio of the baseline system is 0.0132. With the shunts attached to the airfoil, an increase in damping ratio is present for all circuits. The increase in damping ratio for the resistive and resonant circuits is 0.0007 and 0.0014.

A summary of the amplitude reductions for the three stator vanes is given in Table 2.

| Stator Vane | Shunting Circuit | % Strain Reduction at Resonance | % Electrical Reduction at Resonance |
|---|---|---|---|
| | | | |
| SPE | Baseline | -- | -- |
| | Resistive | 8 | 17 |
| | Resonant | 9 | 19 |
| | | | |
| 2PE | Baseline | -- | -- |
| | Resistive | 3 | 6 |
| | Resonant | 6 | 13 |
| | | | |
| LPE | Baseline | -- | -- |
| | Resistive | 8 | 17 |
| | Resonant | 11 | 23 |

Table 2. Summary of Vane Vibration Amplitude Reduction

## SUMMARY & CONCLUSIONS

New techniques for control of flow induced vibrations of low aspect ratio turbomachine blades have been considered. Specifically, the application of shunted piezoelectric elements to provide passive structural damping was investigated by means of a series of experiments performed in the Purdue High Speed Compressor Facility. Piezoelectric elements were bonded to three stator airfoils. The airfoils were excited in a resonant mode by the wakes generated by an upstream rotor. As the wakes drove the resonant airfoil vibrations, the piezoelectrics experienced a strain and in response produced an electric field. Tuned electrical circuits connected to the piezoelectrics as shunts dissipated this electrical energy, with multiple shunting techniques utilized. This electrical energy dissipation and the corresponding reduction in the airfoil mechanical energy resulted in a reduction in the magnitude of the resonant vibrations.

A comparison of the results from the three vanes illustrates that the use of a single large element is more effective than a series of smaller elements for this application. In comparing the SPE and 2PE results, vanes with identical piezoelectric volume but different element configurations, the single large element is more effective than two small elements in converting the kinetic energy of the vibratory motion to electrical energy. Additionally, in comparing the effectiveness of the two large element vanes, SPE vs. LPE, it appears that for the resonant shunt, the effectiveness is strongly coupled to the volume of piezoelectric material present in the system. The LPE vane has a 20% larger piezoelectric volume than the SPE vane and an increase of approximately 20% in amplitude reduction over the SPE vane.

In summary, these passive vibration control experiments demonstrate that shunted piezoelectrics have significant damping capability and could be practical for the elimination or minimization of gas turbine fan and compressor blading flow induced vibrations.

## ACKNOWLEDGMENTS

This research was sponsored, in part, by the Air Force Office of Scientific Research (AFOSR) and the Air Force Research Laboratories (AFRL/PR). This support is most gratefully acknowledged.

## REFERENCES

1. Crawley, E.F. and deLuis, J., 1987, "Use of Piezoelectric Actuators as Elements of Intelligent Structures," *American Institute of Aeronautics and Astronautics Journal* 25 (10), pp. 1373-1385.

2. Poh, S. and Boz, A., 1990, "Active Control of a Flexible Structure Using a Modal Positive Position Feedback Controller," *Journal of Intelligent Material Systems and Structures*, 1(3), pp. 273-288.

3. Bailey, T. and Hubbard, J.E., 1985, "Distributed Piezoelectric-polymer Active Vibration Control of a Cantilever Beam," *American Institute of Aeronautics and Astronautics Journal of Guidance and Control* 8 (5), pp. 605-611.

4. Hollkamp, J.J. and Starchville, T.F., 1994, "A Self-Tuning Piezoelectric Vibration Absorber," *Journal of Intelligent Material Systems and Structures*, 5, pp. 559-566.

5. Hagood, N.W. and von Flotow, A., 1991, "Damping of Structural Vibrations with Piezoelectric Materials and Passive Electrical Networks," *Journal of Sound and Vibration*, 146 (2), pp. 243-268.

6. Jaffe, B., Cook, R. and Jaffe, H., 1971, *Piezoelectric Ceramics*, Academic Press, New York.